A Novel Chloroplast Super-Complex Consisting of the ATP Synthase and Photosystem I Reaction Center

Satarupa Bhaduri[1]† *, Sandeep K Singh[1,] †† *, Whitaker Cohn[2], S. Saif Hasan[1,] †††, Julian P. Whitelegge[2], and William A. Cramer.[1#]

[1]Department of Biological Sciences, Purdue University, West Lafayette, IN 47907;

[2]Pasarow Mass Spectrometry Laboratory, The Jane and Terry Semel Institute for Neuroscience and Human Behavior, David Geffen School of Medicine, University of California/Los Angeles, CA 90024

*authors contributed equally; [#]to whom correspondence should be addressed, (waclab@purdue.edu)

Keywords: ATP synthase, mass spectrometry, native-gel electrophoresis, photosystem I, supercomplex

Abstract. Several 'super-complexes' of individual hetero-oligomeric membrane protein complexes, whose function is to facilitate intra-membrane electron and proton transfer and harvesting of light energy, have been previously characterized in the mitochondrial cristae and chloroplast thylakoid membranes. The latter membrane is reported here to also be the location of an intra-membrane super-complex which is dominated by the ATP-synthase and photosystem I (PSI) reaction-center complexes, defined by mass spectrometry, clear-native PAGE and Western Blot analyses. This is the first documented presence of ATP synthase in a super-complex with the PSI reaction-center located in the non-appressed stromal domain of the thylakoid membrane.

INTRODUCTION

Super-complexes of hetero-oligomeric electron transport membrane protein complexes, formed in the fluid mosaic membrane environment [1,2] have been described in mitochondria [3-6] where their formation has been shown to be facilitated by anionic lipid [3, 7-12]. The chloroplast thylakoid membrane contains four large hetero-oligomeric energy-transducing protein complexes (**Fig. 1**),

for which molecular structure information has been obtained: (i) the photosystem II (PSII) reaction-center complex, responsible for the primary photochemistry associated with water splitting [13]; (ii) the cytochrome b_6f complex [14] which provides the quinol acceptor, electron transfer connection, and trans-membrane proton translocation pathway [15, 16] between the PSII and photosystem I (PSI) reaction centers; (iii) the 561 kDa plant photosystem I (PSI) complex [17, 18] which is responsible for reduction of ferredoxin in the pathway of cyclic electron transport and reduction of $NADP^+$ utilized for CO_2 fixation; and (iv) the 560 kDa ATPase/synthase [19,20]. No super-complex has previously been documented which consists of complexes located in the non-appressed thylakoid region.

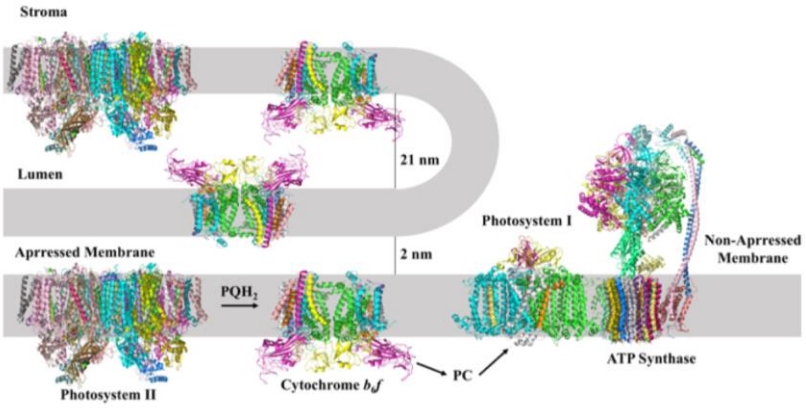

Fig 1. **Distribution of the major intra-membrane energy transducing complexes associated with oxygenic photosynthesis in the appressed (grana) and non-appressed (stroma) thylakoid membranes.** Photosystem II (PSII), photosystem I (PSI), cytochrome b_6f complex, and ATP synthase, with molecular weights of approximately 350, 530, 270 (with FNR), and 560 kDa, respectively. A supercomplex of ATP synthase and photosystem I is implied in the figure by their proximity. Inter-membrane distances are obtained from the references [32, 41].

Bipartite Thylakoid Membrane Structure; Residence of Energy-Transducing Complexes. The chloroplast thylakoid membrane contains the energy transducing light-harvesting and electron-

35 transport protein complexes arranged in two structurally distinct membrane domains, (i) the
36 appressed grana membranes, and (ii) the non-appressed stroma or stroma-facing membrane
37 domain (Fig. 1). The membrane locations of the PSI, PSII, b_6f, and ATPase protein complexes
38 have been discussed in the context of long-range redox communication [21], and the locations in
39 grana and stromal compartments of the redox proteins that function in the 'non-cyclic' electron
40 transport pathway from water to $NADP^+$, and the PSI-linked redox proteins responsible for cyclic
41 electron transport and linked phosphorylation, described [21]. The discovery of super-complexes
42 in thylakoid membranes, which include complexes of the reaction centers with associated light
43 harvesting chlorophyll proteins [22-30] and/or the b_6f complex [31-33] and the electron
44 transport/water-splitting structure [13] has led to an improved perspective on the organization of
45 the membrane protein complexes which support the light harvesting and electron transport-proton
46 translocation functions central to photosynthetic membrane energy transduction.

47 Super-complexes isolated from thylakoid membranes thus far are: (**i**) LHCII: PSII reaction center
48 complexes [22-28]; (**ii**) nano-domains surrounding the PSII reaction center described by atomic
49 force microscopy which are populated by the b_6f complex [34] present in appressed and non-
50 appressed membrane domains [32]; (**iii**) cytochrome b_6f complex from *C. reinhardtii,* to which is
51 bound light harvesting complexes LHCI and LHCII and ferredoxin-NADP+ reductase (FNR),
52 which was obtained under conditions ('state 1- state 2 transition') favoring light energy transfer
53 from the antenna pigment proteins to the PSI reaction center complex [32,33]; (**iv**) the b_6f complex
54 with PSI reaction center complex in *Arabidopsis* and *Chlamydomonas* [32,33]; (**v**) a super-
55 complex of the PSI reaction center and the cytochrome b_6f complex isolated from cold-adapted
56 *C. reinhardtii* [35]; (**vi**) the structures described of the PSI reaction center complex and in
57 association with LHCs from plant sources [29,30]; (**vii**) NDH-associated supercomplexes [32, 36].
58 The presence of the PSI reaction center and ATPase in the edge of the unstacked grana
59 membranes has been documented [37-39].

60 The present study concerns a super-complex that combines the two hetero-oligomeric
61 membrane protein complexes of the non-appressed thylakoid domain, ATP synthase and PSI
62 reaction center, the first membrane protein super-complex in which ATP synthase has a major
63 presence. This result has been documented by the use of high-resolution Orbitrap mass
64 spectrometry to analyze the contribution to the super-complex of multiple major and minor protein
65 components, and clear-native-PAGE, SDS-PAGE, and immuno-blot analysis to identify protein
66 subunits of the component complexes.

67

68 **MATERIALS AND METHODS**

69 ***Purification of (i) Un-crosslinked Super-Complex (Preparations 1 and 2*).** Spinach
70 leaves macerated in darkness in HEPES-KOH pH 7.5, 150 mM NaCl, 5 mM EDTA at 4 °C and
71 sedimented at 4000 x g, were re-suspended in HEPES (4-(2-hydroxyethyl)-1-piperazine-
72 ethanesulfonic acid) -KOH pH 7.5, 15 mM NaCl, 5 mM EDTA, centrifuged at 4,000 x g, and re-
73 suspended in the same medium containing 5 mM NaCl. The chlorophyll concentration of thylakoid
74 membranes was adjusted to 1 mg/ ml, extracted with 1 % DDM, centrifuged at 15,000 x g, the
75 supernatant loaded on a 4-40% sucrose density gradient, and centrifuged at 200,000 x g.

76 ***Purification of (ii) Crosslinked Super-Complex (Preparation 3).*** Spinach leaves
77 macerated in darkness in 50 mM Tris-HCl, pH 7.5, 0.1M NaCl, 0.3 M sucrose, and 1 mM EDTA,
78 at 4 °C and sedimented at 6000 x g, were re-suspended in Tris-HCl, pH 7.5, 0.1 M NaCl, and 1
79 mM EDTA. The suspension was lysed for a second time using the French Press at a pressure of
80 8000 psi. The lysate was centrifuged at 10,000 x g, followed by ultracentrifugation at 160,000 x g
81 for 30 min to separate stacked and unstacked grana thylakoids. The fractions were washed with
82 1 mM EDTA before the chlorophyll concentration was measured and adjusted to 2.5 mg/ml
83 (chlorophyll a/b ratio = 5.4). Membrane proteins were extracted with 1 % β-DDM (β-dodecyl-
84 maltoside), centrifuged at 17,000 x g, the supernatant loaded on a 4-40% sucrose density

85 gradient, and centrifuged at 200,000 x g. The samples were crosslinked by 0.2% glutaraldehyde
86 in the 40% sucrose solution used to make the 10-40% gradient.

87 ***Electrophoretic Analysis*.** Protein bands from the sucrose gradient were fractionated, run on 4-
88 12 % clear-native PAGE, and eight resolved complexes excised for mass spectrometric analysis.
89 The largest band of approximately 1 MDa on the native gel (**Fig. 2B**) is inferred to contain the
90 ATP synthase-PSI super-complex.

91 ***Western Blotting***. Isolated super-complex was assayed on SDS (data not shown) and clear-
92 native PAGE, and transferred to a nitrocellulose membrane, the blot probed with anti-PsaA of PSI,
93 anti-ATP synthase α-subunit, and anti-FNR antibodies obtained from PhytoAb, Inc. (**Fig. 2C,D**
94 **and E**).

95 ***Mass Spectroscopy*.** Mass spectrometry was performed as described previously using nano-
96 liquid chromatography and a bench top Orbitrap mass spectrometer (QE-Plus, Thermo-Fisher
97 Scientific) operated in positive ion mode (nLC-MSMS) [40]. Proteins in native gel-bands were
98 alkylated, digested with trypsin and extracted for nLC-MSMS. The Mascot Search Algorithm
99 (Matrix Science, London, UK) was utilized to identify the significant presence of peptides, using
100 10 ppm mass tolerance on high-resolution precursor MS1 scans, and 20 milli-mass unit tolerance
101 on high-resolution product MS2 scans, obtaining an overall < 5% peptide false discovery rate
102 based upon a reversed sequence decoy search [41]. A spinach database was downloaded from
103 Uniprot (UP000054095). The top twenty Mascot protein scores for each sample were presented
104 representing the most abundant proteins in the sample and minimizing low scoring proteins that
105 are more likely to represent noise (Mascot 'protein' score is the summed score for unique peptides
106 within the sample analysis). A 'complex' score for each of the four major thylakoid protein
107 complexes was generated by adding together the protein scores for the top four highest scoring
108 proteins (or fewer than four if there were fewer than four proteins from that complex in the twenty
109 highest scoring proteins). The top twenty proteins were chosen as a cutoff because proteins below

110 this threshold have protein scores around 10% or less of the highest scoring proteins and thus
111 are more likely to be in the 'noise' fraction [32].

112 ***Assay of ATPase Activity*.** The "ADP-Glo" kit (Promega, Wisconsin) was used to measure
113 hydrolysis of ATP to ADP and inorganic phosphate by ATPase. ATP (0.4 mM) was added to the
114 super-complex fraction in the presence of buffer (50 mM Tris-HCl, 5 mM Mg^{2+}, and BSA) at room
115 temperature, incubated for 15 min, followed by the addition of "ADP-Glo reagent" and incubation
116 at room temperature (40 min) to consume unused ATP. The reaction mixture was then incubated
117 with the 'detection reagent' to convert ADP to ATP, measured by the reaction of luciferase/luciferin,
118 and the luminescence recorded in a spectral band centered at 560 nm, utilizing a Spectramax
119 Luminometer (Molecular Devices, CA)**.**

120 ***Fluorescence Emission Spectroscopy*.** Fluorescence measurements were made with a
121 FluoroMax 3 Fluorimeter (Horriba-Yvon Inc.), using a 3 x 3 mm quartz microcell with 0.3 ml
122 volume. FAD containing the super-complex fraction in 10 mM HEPES buffer, pH 7.5, 0.5 mM
123 EDTA, 2 mM DDM, 10 % sucrose. Fluorescence was excited at 460 nm, and emission spectra
124 collected in a 500-580 nm spectral interval, with a stepping increment of 1 nm and a 0.1 sec
125 integration time. Excitation spectra were measured from 420 – 500 nm using an emission band
126 interval centered at 530 nm. Difference spectra were obtained by measuring the fluorescence in
127 the presence and absence of sodium dithionite, the latter a reductant with a redox potential
128 negative enough to fully reduce the flavin in FNR, thus effectively eliminating its absorbance and
129 resulting fluorescence.

130

131 **RESULTS**

132 ***A unique super-complex from thylakoid membranes; electrophoretic and immuno-blot***
133 ***analysis*.** The super-complex was isolated from spinach thylakoid membranes by detergent

extraction followed by sucrose density gradient centrifugation (**Fig. 2A**, marked as “SC”), and the approximate size was determined on a 4–12 % clear-native gel (**Fig. 2B**).

The presence of ATP synthase, PS I and FNR was confirmed by Western blot analyses using antibodies raised against the *Arabidopsis* ATP synthase α-subunit (55 kDa) (**Fig. 2C**), the 60 kDa PsaA subunit of PSI (**Fig. 2D**), and FNR (36 kDa) (**Fig. 2E**).

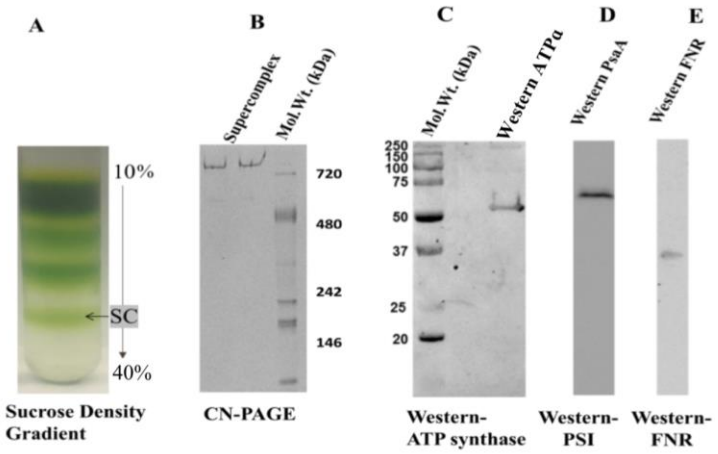

Fig 2. **Purification and characterization of the PSI-ATP synthase super-complex**. **(A)** 4-40 % sucrose density gradient of spinach thylakoid membrane extract. Super-complex (SC), marked by the arrow, is separated for further characterization. **(B)** 4-12 % Clear Native PAGE of the super-complex fraction isolated from the sucrose gradient and stained with Coomassie Brilliant Blue R-250. (**C, D, E**) Western blots of super-complex using 12 % SDS-PAGE probed with antibodies raised against **(C)** α-subunit (55 kDa) of *Arabidopsis* ATP synthase, **(D)** PsaA subunit (60 kDa) of PSI, and **(E)** ferredoxin-NADPH oxidoreductase (FNR).

Mass Spectrometry. High-resolution mass spectrometry of the isolated 1 MDa super-complex from spinach chloroplast thylakoid membranes (**Table 1**) revealed the presence of ATP synthase (0.56 MDa), Photosystem I (0.53 MDa). Polypeptide components derived from the 1MDa band in **Fig. 2B**, were identified after in-gel digestion of the native gel-band and tandem mass spectrometry with database searching constrained by a specified high statistical confidence threshold, as described in *Methods*, and summarized in **Table 1A, B**. Presence of ATP synthase

155 and Photosystem I were identified with high statistical confidence by multiple polypeptides.
156 Notably absent were Photosystem II (trace amounts of PsbB were detected in 1 preparation,
157 assumed to represent contamination), and cytochrome b_6f complex polypeptides. Other
158 components that were detected consistently were the polypeptides FtsH and FtsH2, Lhca3.1 (a
159 known PSI chlorophyll a/b binding protein) and ferredoxin-NADPH oxidoreductase (FNR) that was
160 confirmed by Western blot (**Fig. 2E**). A calcium-sensing receptor was found in 2/3 preparations
161 and rubisco activase was found with a high score after crosslinking. Because of differential
162 recovery of larger versus smaller subunits and peptides derived from them it is not possible to
163 infer polypeptide stoichiometry from these measurements.

164 **Table 1A. Identification of Twenty Highest Scoring Proteins in Three Super-Complex**
165 **Preparations**

Preparation 1	**Score**	**Preparation 2**	**Score**	**Preparation3 (crosslinked)**	**Score**
AtpB	2844	AtpB	2106	FtsH	4138
PsaB	2055	PsaB	2006	Rubisco activase [p]	4065
AtpA	1295	PsaD	1343	PsaB	3707
PsaD[a]	1261	AtpA	861	AtpB	3573
FtsH[b]	753	Lhca3.1	694	FtsH2	3281
Lhca3.1[c]	677	FNR	604	NadH1[q]	2548
Lhca6A[d]	664	PsbB	517	PsaD	2135
FNR	652	PsaF	492	NdhB2	1892
AtpG[e]	634	PsaA	471	Lhca3.1	1848
FtsH2[f]	613	PsaC	450	AtpA	1829
AtpE	591	AtpD	449	PsaG	1713
NdhB2[g]	559	FtsH2	439	Calcium-sensing receptor	1584
PsaC	503	PsaE[m]	435	PsaA	1337

PsaA	493	Lhca(7)	431	PsaE	1094
Lhca(7)[h]	449	PsaG	349	AtpG	1074
AtpD[i]	444	Lhca6A	348	ClpA_CD4B[r]	1066
PsaF[j]	442	AtpE	334	NADH1_13B[s]	1012
calcium-sensing recep.[k]	422	FtsH	330	□_carbonic anhydr. 1[t]	1005
RbLrubisco	409	Lhca4[n]	310	Lhca4	912
PsaG[l]	371	P31853.2[0]	301	Lhca6A	808

By BLAST homology, PsaD, tr|A0A0K9R886|A0A0K9R886_SPIOL

By BLAST homology, FtsH, tr|A0A0K9RFL8|A0A0K9RFL8_SPIOL

By BLAST homology, Lhca3.1, tr|A0A0K9R1K7|A0A0K9R1K7_SPIOL

By BLAST homology, Lhca6A, tr|A0A0K9RRT4|A0A0K9RRT4_SPIOL

By BLAST homology, AtpG, tr|A0A0K9QPJ7|A0A0K9QPJ7_SPIOL

By BLAST homology, FtsH2, tr|A0A0K9RD58|A0A0K9RD58_SPIOL

By BLAST homology, NdhB2, tr|A0A0K9QKT8|A0A0K9QKT8_SPIOL

By BLAST homology, Lhca(7), tr|A0A0K9RU56|A0A0K9RU56_SPIOL

By BLAST homology, AtpD, tr|A0A0K9RXF7|A0A0K9RXF7_SPIOL

By BLAST homology, PsaF, tr|A0A0K9RVH9|A0A0K9RVH9_SPIOL

By BLAST homology, calcium-sensing receptor, tr|A0A0K9R5V6|A0A0K9R5V6_SPIOL

By BLAST homology, PsaG, tr|A0A0K9RHQ2|A0A0K9RHQ2_SPIOL

By BLAST homology, PsaE, tr|A0A0K9RHN1|A0A0K9RHN1_SPIOL

By BLAST homology, Lhca4, tr|A0A0K9R772|A0A0K9R772_SPIOL

By BLAST homology, ATPase b', tr|A0A0K9QQW2|A0A0K9QQW2_SPIOL

By BLAST homology, Rubisco activase, tr|A0A0K9Q765|A0A0K9Q765_SPIOL

By BLAST homology, NadH1, tr|A0A0K9QED7|A0A0K9QED7_SPIOL

By BLAST homology, ATP-dependent Clp protease ATP-binding subunit ClpA homolog CD4B, tr|A0A0K9QTC9|A0A0K9QTC9_SPIOL

By BLAST homology, NadH1_13B, tr|A0A0K9Q7H2|A0A0K9Q7H2_SPIOL

187 By BLAST homology, □_carbonic anhydr. 1, tr|A0A0K9RNJ7|A0A0K9RNJ7_SPIOL

188

189 **Table 1B. Major Thylakoid Complexes in Supercomplex.**

190 4 highest scores for each complex component added together.

Complex	**Prep. 1**	**Prep.2**	**Prep.3 (crosslinked)**
ATPase	5364	3750	6476
PSI	4312	4312	8892
b_6f	0	0	0
PSII*	0	517[c]	0

191 *Minor contamination in by PSII.

192

193 The presence of FNR was confirmed through Western blot analysis using an anti-FNR antibody
194 probe (**Fig. 2E**), and determination of fluorescence excitation and emission spectra that are
195 characteristic of FAD [42] (**Fig. 3**). No polypeptides from the cytochrome *b_6f* complex were
196 detected at the stringency used.

197

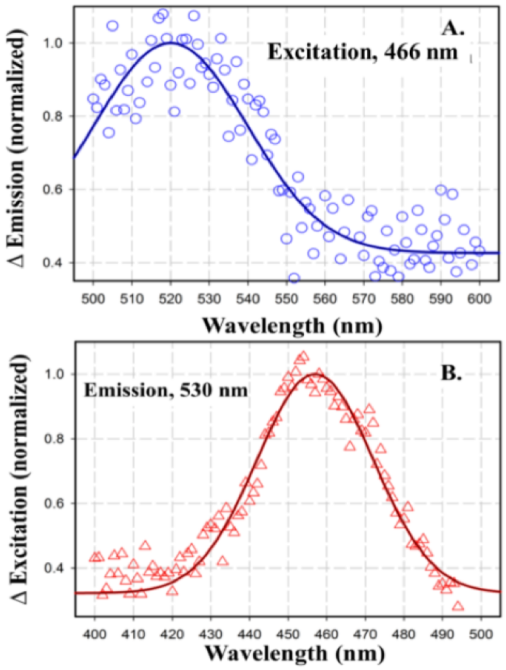

Figure 3. Difference fluorescence emission (top) and excitation (bottom) spectra of the 'super-complex;' measured with a FluoroMax 3 Fluorimeter (Horiba-Yvon Inc.). (**A)** Emission spectra measured between 500 – 600 nm. Stepping increment, 1 nm; Integration time, 0.1 sec; Excitation, 466 nm; bandwidth 5 nm for excitation and emission. (**B)** Excitation spectra measured in 400–500 nm range, measuring the emission at its 530 nm peak. Spectra of undiluted sample were measured in a quartz microcell, 3 x 3 mm, volume, 0.3 ml (Starna Cells) before and after addition of dithionite grains. Difference spectra were obtained by subtraction of spectra, i. e., 'oxidized–reduced,' measured before and after addition of dithionite.

Presence of FNR in the Super-Complex. The presence of FNR in the spinach super complex was confirmed from fluorescence emission and excitation spectra produced by the isoalloxazine moiety of FAD (**Figs. 3A, B**). The super-complex, suspended in 10 mM HEPES buffer, pH 7.5, and 0.5 mM EDTA, 2 mM DDM, 10 % sucrose, was excited at 460 nm and emission spectra were acquired over the wavelength range 500-600 nm. The difference emission spectrum, calculated with and without the strong reductant, sodium dithionite, showed an emission maximum in the oxidized state at 530 nm, which is characteristic of the presence of flavin [42]. A similar conclusion was reached from the difference excitation spectra measured with and without sodium dithionite

over the 400-500 nm range using emission at 530 nm. The excitation spectrum showed maximum at 460 nm, characteristic of oxidized flavin [42]. Spectra are normalized to unit emission intensity.

ATPase Activity. The F1-ATPase component in the super-complex demonstrated *in vitro* ATP hydrolysis, as described in *Methods*. The "ADP-Glo kit" (Promega) was used to provide a qualitative measure of ATP hydrolysis, which was dependent on the presence of the PSI-ATPase-FNR super-complex (**Table 2**). ATP hydrolysis was measured by addition of 0.4 mM ATP to the super-complex fraction in the buffer containing 50 mM Tris-HCl, 5 mM Mg^{2+}, and 0.1 mg/ml BSA).

Table 2. ATPase Activity of the Super-Complex. As described in *Methods*, kinase activity was measured qualitatively through luciferase emission in the positive control (buffer and 0.4 mM ADP); negative control (buffer and ATP (0.4 mM) and the purified super-complex in buffer and 0.4 mM ATP.

Sample	**Chemiluminescent Signal (cpm)**
+ADP (positive control)	$(3.1 \pm 2) \times 10^6$
+ATP (negative control)	$(5.5 \pm 1.2) \times 10^2$
+ Supercomplex	$(4.4 \pm 0.6) \times 10^5$

DISCUSSION

Several super-complexes of PSI with thylakoid complexes have previously been described [17,18, 29, 30], but a complex with ATP synthase has thus far been absent. These authors defined the super-complex based upon the ability to visualize the complex using cryo-electron microscopy. In the present case it has not been possible to preserve the PSI-ATP synthase complex during the freezing process for cryo-EM. Consequently, we do not include an EM image of this super-complex in this study. Alternatively, classical biochemical techniques show this super-complex running as a discrete band in sucrose-gradient centrifugation and as a ~1 MDa band on a native gel combined with a modern description of the major components of the super-complex by high-resolution mass spectrometry.

The identity of the PSI-ATP synthase super-complex is supported by the facts that (i) the super-complex band is the densest, implying a higher protein/lipid content than other thylakoid super-complexes consistent with the presence of the ATP synthase which contains no pigments; (ii) the molecular weight observed by native gel electrophoresis of ~1 MDa is consistent with an equimolar mixture of PSI [17,18] (MW= 561 kDa) and ATP synthase (MW = 560 kDa) [19,20], and no other complex.

Modern mass spectrometry using high-resolution precursor- and production scans in tandem MS protein identification underscores current proteomics [44]. In-gel analysis of bands on native gels is relatively uncommon compared to bands on SDS gels. In fact, the number of tryptic peptides derived from the subunits of a super-complex, far exceeds that expected from trypsin treatment of a single protein. The modern mass spectrometer combined with reverse-phase chromatography provides a powerful tool to analyze a heterogenous mixture of peptides to determine the super-complex. Integral membrane proteins with large extrinsic domains yield abundant peptides that are easily recoverable in the in-gel procedure yielding very high relative abundance 'scores' where these subunits are present. Thus, ATP synthase and PSI with very high scores are identified, based on the four highest scoring polypeptides underlying our conclusion that these two complexes are the only complexes within this super-complex (**Table 1B**). PSII and cytochrome b_6f components are easily identified in other bands from the sucrose gradient (not shown) but not in the densest band representing the super-complex as described. Small subunits with a large proportion of transmembrane sequence are poorly represented in this type of analysis [45] and were not seen in this analysis. Intact protein analysis is better suited for full subunit coverage, as reported in 2002 [46] and would be well suited to detect all the subunits in the supercomplex. Native intact supercomplex mass spectrometry would be most desirable as it addresses stoichiometry [47], but it as yet unavailable for this preparation.

Mass spectrometry also showed the presence of other proteins that might be harder to define by cryo-EM, reliably identifying FtsH and FtsH2, Lhca3A and FNR. Initial studies on these components have documented the presence of FNR.

This is the first instance of detection of a photosynthetic super-complex which contains the ~560 kDa ATP synthase protein complex. Localized coupling of the electron transport system and ATP synthesis by super-complex formation in mitochondria has been proposed [48]. It has been suggested that the oxidative phosphorylation system in respiratory systems can operate in two states: via utilization of (i) the bulk phase trans-membrane electrochemical potential gradient [48], or (ii) protons localized in the membrane that are accessible to the active site chemistry [49]. In the present study, the occurrence of ATP synthase in association with the PSI reaction-center complex, suggests the possibility of a relatively localized coupling between (i) ATP synthesis and the transmembrane electrical potential generated in the PSI reaction center, and/or (ii) a localized domain of carbon dioxide fixation.

The isolated complex dominated by the presence of PSI and ATP synthase is also associated with a number of proteins like the ATP dependent, membrane anchored zinc metalloprotease FtsH, FNR and Rubisco Activase. FtsH has been implicated in chloroplast biogenesis and repair of photosystem II under high light conditions [50]. It has been demonstrated that FtsH, localized in the stroma lamellae, is critical for the biogenesis of PSI complex under normal light conditions [51]. In bacteria FtsH is responsible for regulating ATP synthase biogenesis [52]. However, such a function has not yet been documented in the plant system.

Previous studies have shown that a Chl a/b ratio of 4.6 in the stroma lamellae isolated from spinach leaves, had a PSI/PSII ratio of ~3 [53]. In the current preparation, a chlorophyll a/b ratio of 5.4 was measured in the membrane fraction, which indicates that the super-complex PSI-ATPase containing has been derived from a PSI enriched stroma lamellae membrane. A high

relative abundance of Lhca 3.1, a light harvesting protein associated with PSI [54], as determined by mass spectrometry, also confirms a major presence of photosystem I in the super-complex.

The flavoenzyme, ferredoxin-$NADP^+$ reductase (FNR), found in both soluble and thylakoid membrane associated forms, has been proposed to define the photosynthetic electron transport pathway [55]. PSI bound FNR or soluble stromal FNR facilitates linear electron flow, while under reduced conditions, FNR associates with the cytochrome b_6f complex and promotes cyclic electron flow [56]. The presence of FNR in the super-complex has been confirmed by mass spectrometry (**Table1A**), Western Blot (**Fig. 2E**) and difference fluorescence spectroscopy (**Fig. 3**). A third protein, rubisco activase, found associated with the high molecular weight crosslinked band containing PSI and ATP synthase (Preparation 3), interacts with Rubisco to release the bound inhibitors in an ATP dependent fashion and hence, initiates the CO_2 fixation cycle [57].

AUTHOR INFORMATION

Corresponding Author

*e-mail: waclab@purdue.edu; telephone: (765)-494-4956

Present Addresses

†Department of Cellular and Developmental Biology and Department of Biosciences, University of California, San Diego, 9500 Gilman Drive, La Jolla, CA 92093; †† Department of Biological Chemistry & Molecular Pharmacology, Harvard Medical School, 240 Longwood Avenue, Boston MA, 02115; ††† Department of Biochemistry and Molecular Biology, University of Maryland School of Medicine, 108 N. Greene St., Baltimore, MD 21201 AND Center for Biomolecular Therapeutics (CBT), 9600 Gudelsky Drive, Rockville, MD 20850

Author Contributions. Project proposed by SKS and WAC. Super-complex isolation and biochemical characterization done by SKS and SB. Mass spectrometry analyses done by JPW. SSH contributed to the experimental design. Manuscript written by SB, JPW, and WAC.

ABBREVIATIONS. CN- and SDS-PAGE, clear native- and sodium dodecyl sulfate-polyacrylamide gel electrophoresis; cpm, counts/min; cyt, cytochrome; DDM, n-dodecyl-β-D-malto-pyranoside; FNR, ferredoxin-$NADP^+$ reductase; EM, electron microscopy; FtsH, filamentous, temperature-sensitive ATP-dependent protease; HRP, horse radish peroxidase; LHC, light harvesting complex; Mr, relative molecular weight; PAGE, polyacrylamide gel electrophoresis; pdb, protein data bank; PSI, PSII, photosystems I, II.

ACKNOWLEDGMENTS.

We thank S. D. Zakharov, S. Puthiyaveetil, R. Morgan-Kiss, and I. Kalra for helpful discussions, and S. Naurin for technical support. Studies were supported by Dept. of Energy/Basic Energy Sciences/Photosynthetic Systems grant DE-SC00118238, the Henry Koffler Distinguished Professorship (WAC), and NIHDK-063491 (JPW).

REFERENCES

1. Singer SJ and Nicholson GL. The fluid mosaic model of the structure of cell membranes. Science 1972;175*:* 720-731.
2. Engelman DM. Membranes are more mosaic than fluid, Nature 2005; 438: 578-580.
3. Pfeiffer K, Gohil V, Stuart RA, Hunte C, Brandt U, Greenberg ML, Schägger H. Cardiolipin stabilizes respiratory chain supercomplexes, Journal of Biological Chemistry 2003; 278: 52873-52880.
4. Genova ML, Lenaz G. Functional role of mitochondrial respiratory supercomplexes, Biochimica et Biophysica Acta (BBA) - Bioenergetics 2014;1837: 427-443.
5. Sousa JS, D'Imprima E, Vonck J. Mitochondrial respiratory chain complexes, in *membrane protein complexes: structure and function* (Harris, J. R., and Boekema, E. J., Eds.) 2018; pp. 167-227, Springer Singapore, Singapore.
6. Davies KM, Blum TB, Kühlbrandt W. Conserved in situ arrangement of complex I and III_2 in mitochondrial respiratory chain supercomplexes of mammals, yeast, and plants. Proceedings of the National Academy of Sciences 2018; 115: 3024-3029.
7. Wenz T, Hielscher R, Hellwig P, Schagger H, Richers S, Hunte C. Role of phospholipids in respiratory cytochrome bc_1 complex catalysis and supercomplex formation Biochim. Biophys. Acta 2009; 1787: 609-616.
8. Mileykovskaya E, Dowhan W. Cardiolipin-dependent formation of mitochondrial respiratory supercomplexes, Chemistry and Physics of Lipids 2014; 179: 42-48.
9. Arnarez C, Marrink SJ, Periole X. Molecular mechanism of cardiolipin-mediated assembly of respiratory chain supercomplexes, Chemical Science 2016; 7: 4435-4443.
10. Blaza JN, Serreli R, Jones AJ, Mohammed K, Hirst J. Kinetic evidence against partitioning of the ubiquinone pool and the catalytic relevance of respiratory chain supercomplexes. Proceedings of the National Academy of Sciences of the United States of America 2014; 111*:* 15735-15740.
11. Bottinger L, Horvath SE, Kleinschroth T, Hunte C, Daum G, Pfanner N, Becker T. Phosphatidyl-ethanolamine and cardiolipin differentially affect the stability of mitochondrial respiratory chain supercomplexes, J Mol Biol 2012; 423*:* 677-686.
12. Arnarez C, Marrink SJ, Periole X. Identification of cardiolipin binding sites on cytochrome c oxidase at the entrance of proton channels, Sci Rep 2013; 3: 1263.
13. Umena Y, Kawakami K, Shen JR, Kamiya, N. Crystal structure of oxygen-evolving photosystem II at a resolution of 1.9 A, Nature 2011; 473*:* 55-60.

14. Hasan SS, Cramer WA. Internal lipid architecture of the hetero-oligomeric cytochrome b_6f complex. Structure 2014; 22: 1008-1015.

15. Hasan SS, Yamashita E, Baniulis D, Cramer WA. Quinone-dependent proton transfer pathways in the photosynthetic cytochrome b_6f complex. Proc Natl Acad Sci. 2013; 110: 4297–4302.

16. Shikanai T, Yamamoto H. Contribution of cyclic and pseudo-cyclic electron transport to the formation of proton motive force in chloroplasts. Molecular Plant 2017; 10: 20-29.

17. Mazor Y, Borovikova A, Caspy I, Nelson N. Structure of the plant photosystem I supercomplex at 2.6 A resolution. Nature Plants 2017; 3: 17014.

18. Caspy I, Nelson N. Structure of the plant photosystem I. Biochemical Society Transactions 2018; 46(2): 285-294.

19. Hahn A, Vonck J, Mills DJ, Meier T, Kühlbrandt W. Structure, mechanism, and regulation of the chloroplast ATP synthase, Science 2018; 360: aat4318.

20. Kühlbrandt W. Structure and mechanisms of f-type ATP synthases. Annual Review of Biochemistry 2019; 88: 515-549.

21. Anderson JM. Lateral heterogeneity of plant thylakoid protein complexes: early reminiscences. Philos Trans R Soc Lond B Biol Sci 2012; *367:* 3384-3388.

22. Joliot P, Joliot GN. Regulation of cyclic and linear electron flow in higher plants, Proceedings of the National Academy of Sciences of the United States of America 2011; 108 13317-13322.

23. Crepin A, Santabarbara S, Caffarri S. Biochemical and spectroscopic characterization of highly stable photosystem ii supercomplexes from *Arabidopsis*, The Journal of biological chemistry 2016; 291: 19157-19171.

24. van Bezouwen LS, Caffarri S, Kale RS, Kouril R, Thunnissen AWH, Oostergetel GT, Boekema EJ. Subunit and chlorophyll organization in the plant photosystem II supercomplex, Nature Plants 2017; 3: 17080.

25. Wei X, Su X, Cao P, Liu X, Chang W, Li M, Zhang X, Liu Z. Structure of spinach photosystem II–LHCII supercomplex at 3.2 Å resolution, Nature 2016; 534: 69.

26. Su X, Ma J, Wei X, Cao P, Zhu D, Chang W, Liu Z, Zhang X, Li, M. Structure and assembly mechanism of plant $C_2S_2M_2$-type PSII-LHCII supercomplex. Science 2017; 357: 815.

27. Sheng X, Liu X, Cao P, Li M, Liu Z. Structural roles of lipid molecules in the assembly of plant PSII-LHCII supercomplex. Biophys Rep 2018; 4: 189-203.

28. Pi X, Zhao S, Wang W, Liu D, Xu C, Han G, Kuang T, Sui SF, Shen JR. The pigment-protein network of a diatom photosystem II–light-harvesting antenna supercomplex, Science 2019; 365, eaax4406.

29. Suga M, Qin X, Kuang T, Shen JR. Structure and energy transfer pathways of the plant photosystem I-LHCI supercomplex. Current Opinion in Structural Biology 2016; 39: 46-53.

30. Pan X, Ma, J, Su X, Cao P, Chang W, Liu Z, Zhang X, Li M.Structure of the maize photosystem I supercomplex with light-harvesting complexes I and II. Science 2018; 360: 1109.

31. Iwai M, Takizawa K, Tokutsu R, Okamuro A, Takahashi Y, Minagawa J. Isolation of the supercomplex that drives cyclic electron flow in photosynthesis. Nature 2010; 464: 1210-1213.

32. Yadav KN, Semchonok DA, Nosek L, Kouril R, Fucile G, Boekema EJ, Eichacker LA. Supercomplexes of plant photosystem I with cytochrome b_6f, light-harvesting complex II and NDH, Biochim Biophys Acta 2017; 1858*:* 12-20.

33. Steinbeck J, Ross IL, Rothnagel R, Gäbelein P, Schulze S, Giles N, Ali R, Drysdale R, Sierecki E, Gambin Y, Stahlberg H, Takahashi Y, Hippler M, Hankamer B. Structure of a PSI–LHCI–cyt b_6f supercomplex in *Chlamydomonas reinhardtii* promoting cyclic electron flow under anaerobic conditions. Proceedings of the National Academy of Sciences 2018; 115: 10517-10522.

34. Johnson MP, Vasilev C, Olsen JD, Hunter CN. Nanodomains of cytochrome b_6f and photosystem II complexes in spinach grana thylakoid membranes, Plant Cell 2014; 26: 3051-3061.

35. Szyszka-Mroz B, Pittock P, Ivanov AG, Lajoie G, Huner NP. The Antarctic psychrophile *Chlamydomonas sp*. UWO 241 preferentially phosphorylates a photosystem I-cytochrome b_6f supercomplex, Plant physiology 2015; 169: 717-736.

36. Kato Y, Sugimoto K, Shikanai T. NDH-PSI supercomplex assembly precedes full assembly of the ndh complex in chloroplast, Plant Physiology 2018;176: 1728.

37. Kaftan D, Brumfeld V, Nevo R, Scherz A, Reich Z. From chloroplasts to photosystems: in situ scanning force microscopy on intact thylakoid membranes. The EMBO journal 2002; 21: 6146-6153.

38. Puthiyaveetil S, Tsabari O, Lowry T, Lenhert S, Lewis RR, Reich Z, Kirchhoff H. Compartmentalization of the protein repair machinery in photosynthetic membranes, Proceedings of the National Academy of Sciences of the United States of America 2014; 111: 15839-15844.

39. Kirchhoff H, Li M, Puthiyaveetil S. Sublocalization of cytochrome b_6f complexes in photosynthetic membranes. Trends in Plant Science 2017; 22: 574-582.

40. Ding L, Xie F, Zhao M, Wang S, Xie J, Xu G. Rapid quantification of sucrose esters in oriental tobacco by liquid chromatography-ion trap mass spectrometry, Journal of Separation Science 2007; 30: 35-41.

41. Elias JE, Gygi SP.Target-decoy search strategy for mass spectrometry-based proteomics, Methods Mol Biol 2010; 604: 55-71.

42. Maeda M, Hamada D, Hoshino M, Onda Y, Hase T, Goto Y. Partially folded structure of flavin adenine dinucleotide-depleted Ferredoxin-$NADP^+$ Reductase with residual $NADP^+$ binding domain. Journal of Biological Chemistry 2002; 277: 17101-17107.

43. Vossen KM, Fried MG. Sequestration stabilizes lac repressor–DNA complexes during gel electrophoresis. Analytical Biochemistry 1997; 245: 85-92.

44. Mann M,Kelleher NL.Precision proteomics: the case for high resolution and high mass accuracy, Proceedings of the National Academy of Sciences of the United States of America 2008; 105: 18132-18138.

45. Souda P, Ryan CM, Cramer WA, Whitelegge J. Profiling of integral membrane proteins and their post translational modifications using high-resolution mass spectrometry, Methods 2011; 55: 330-336.

46. Whitelegge JP, Zhang H, Aguilera R, Taylor RM, Cramer WA. Full subunit coverage liquid chromatography electrospray ionization mass spectrometry (lcms+) of an oligomeric membrane protein, cytochrome b_6f complex from spinach *and the* cyanobacterium *Mastigocladus Laminosus.* Mol. Cell Proteomics 2002; *1*, 816-827.

47. Robinson CV. Mass spectrometry: From plasma proteins to mitochondrial membranes. Proc Natl Acad Sci U S A. 2019 ;116(8): 2814-2820.

48. Mitchell P. Coupling of phosphorylation to electron and hydrogen transfer by a chemi-osmotic type of mechanism. Nature 1961; 191: 144-148.

49. Williams RJP. Possible functions of chains of catalysts, Journal of Theoretical Biology 1961;1: 1-17.

50. Kato Y, Sakamoto W. FtsH protease in the thylakoid membrane: physiological functions and the regulation of protease activity, Frontiers in Plant Science 2018; 9: 855-855.

51. Järvi S, Suorsa M, Tadini L, Ivanauskaite A, Rantala S, Allahverdiyeva Y, Leister D, Aro EM. Thylakoid-bound FtsH proteins facilitate proper biosynthesis of photosystem I, Plant physiology 2016;171: 1333-1343.

52. Deckers-Hebestreit G. Assembly of the *Escherichia coli*; F_0F_1ATP synthase involves distinct subcomplex formation, Biochemical Society Transactions 2013; 41: 1288.

460 53. Danielsson R, Albertsson PÅ, Mamedov F, Styring S. Quantification of photosystem I and
461 II in different parts of the thylakoid membrane from spinach, Biochimica et Biophysica Acta (BBA)
462 - Bioenergetics 2004; 1608: 53-61.
463 54. Ozawa SI, Bald T, Onishi T, Xue H, Matsumura T, Kubo R, Takahashi H, Hippler M,
464 Takahashi Y.Configuration of Ten Light-Harvesting Chlorophyll a/b Complex I Subunits in
465 *Chlamydomonas reinhardtii* Photosystem I, Plant Physiology 2018; 178: 583-595.
466 55. Mosebach, L, Heilmann C, Mutoh R, Gäbelein P, Steinbeck J, Happe T, Ikegami T, Hanke
467 G, Kurisu G, Hippler M. Association of Ferredoxin:NADP+ oxidoreductase with the photosynthetic
468 apparatus modulates electron transfer in *Chlamydomonas reinhardtii*, Photosynthesis Research
469 2017; 134: 291-306.
470 56. Joliot P, Joliot A. Cyclic electron flow in C3 plants, Biochimica et Biophysica Acta (BBA) -
471 Bioenergetics 2006;1757: 362-368.
472 57. Keown JR, Griffin MD, Mertens HD, Pearce FG. Small oligomers of ribulose-bisphosphate
473 carboxylase/oxygenase (rubisco) activase are required for biological activity, Journal of Biological
474 Chemistry 2013; 288: 20607-20615.

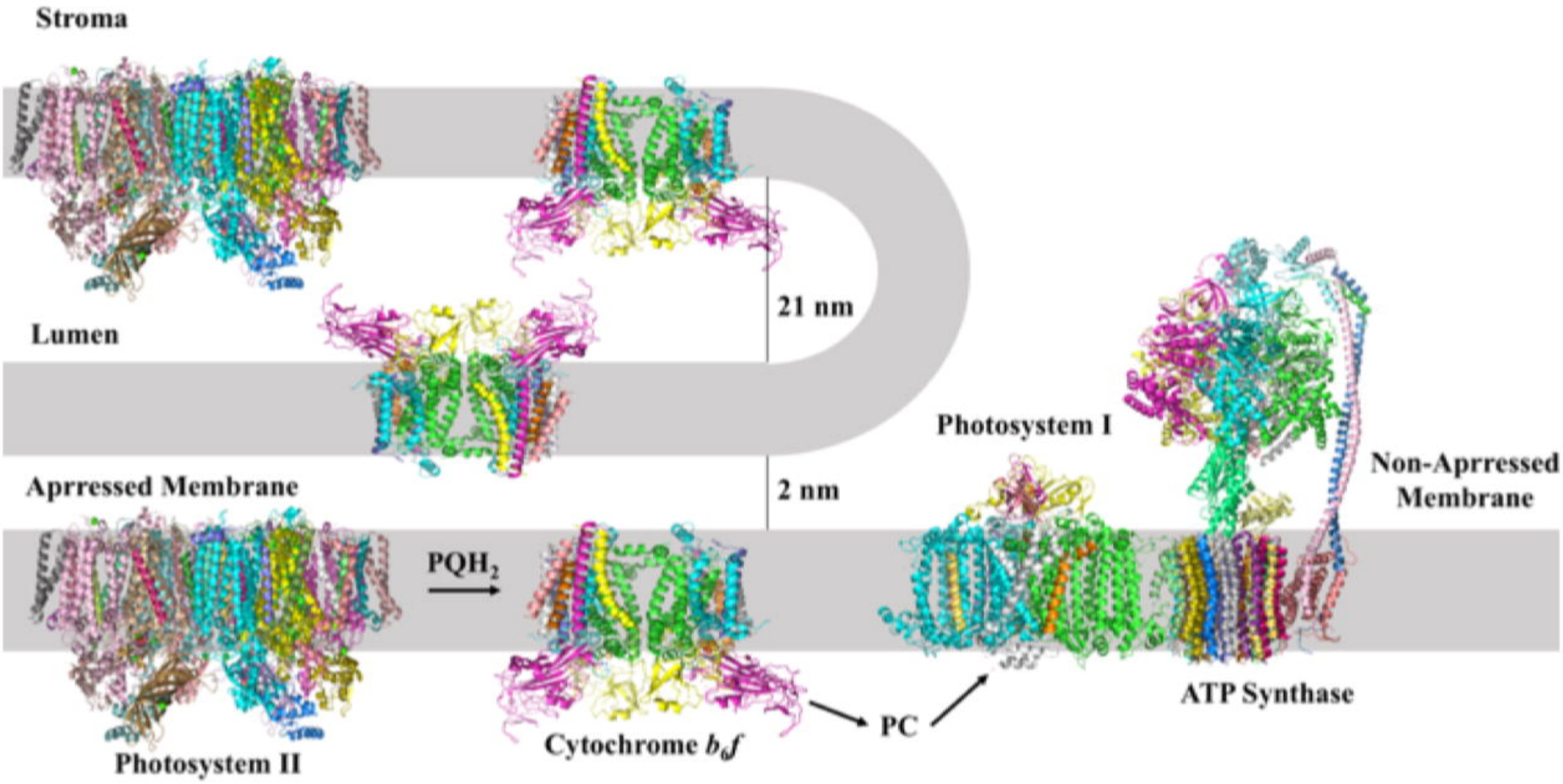
Stroma
Lumen
21 nm
Aprressed Membrane
2 nm
Photosystem I
Non-Aprressed Membrane
PQH$_2$
Photosystem II
Cytochrome b_6f
PC
ATP Synthase

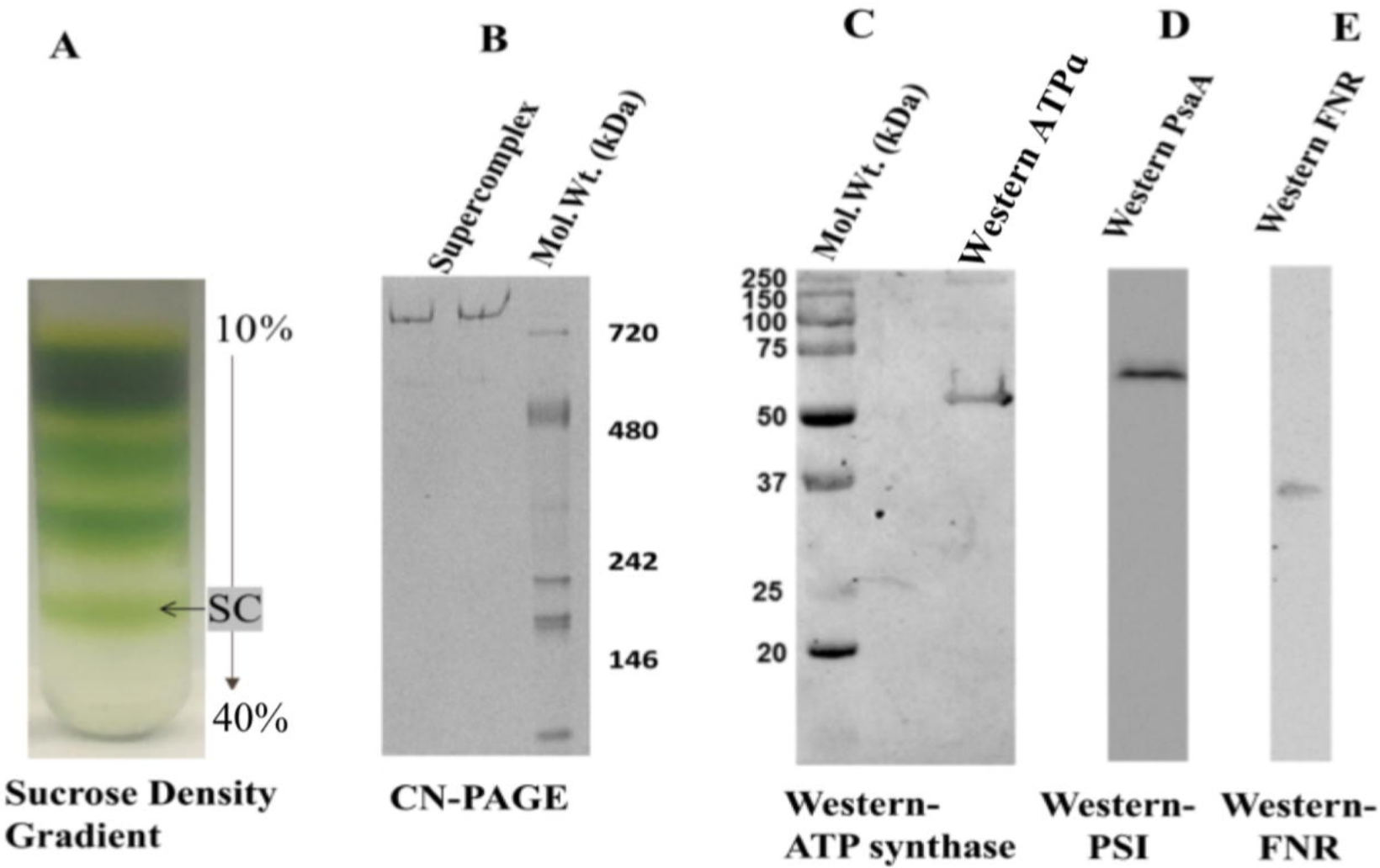
A
B
C
D
E
Supercomplex
Mol.Wt. (kDa)
Mol.Wt. (kDa)
Western ATPα
Western PsaA
Western FNR
10%
SC
40%
720
480
242
146
250
150
100
75
50
37
25
20
Sucrose Density Gradient
CN-PAGE
Western-ATP synthase
Western-PSI
Western-FNR

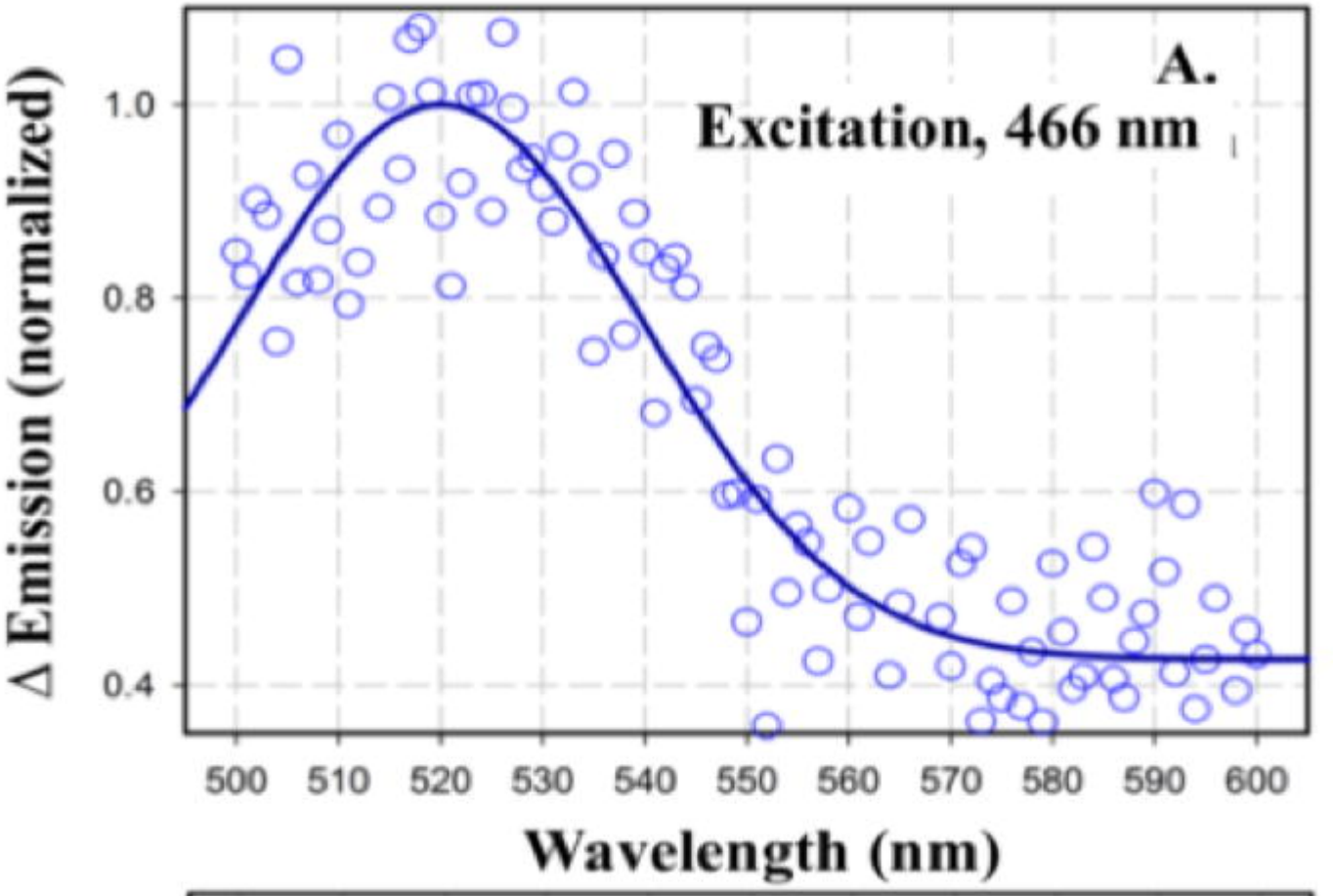
A.
Excitation, 466 nm
Δ Emission (normalized)
1.0
0.8
0.6
0.4
500
510
520
530
540
550
560
570
580
590
600
Wavelength (nm)

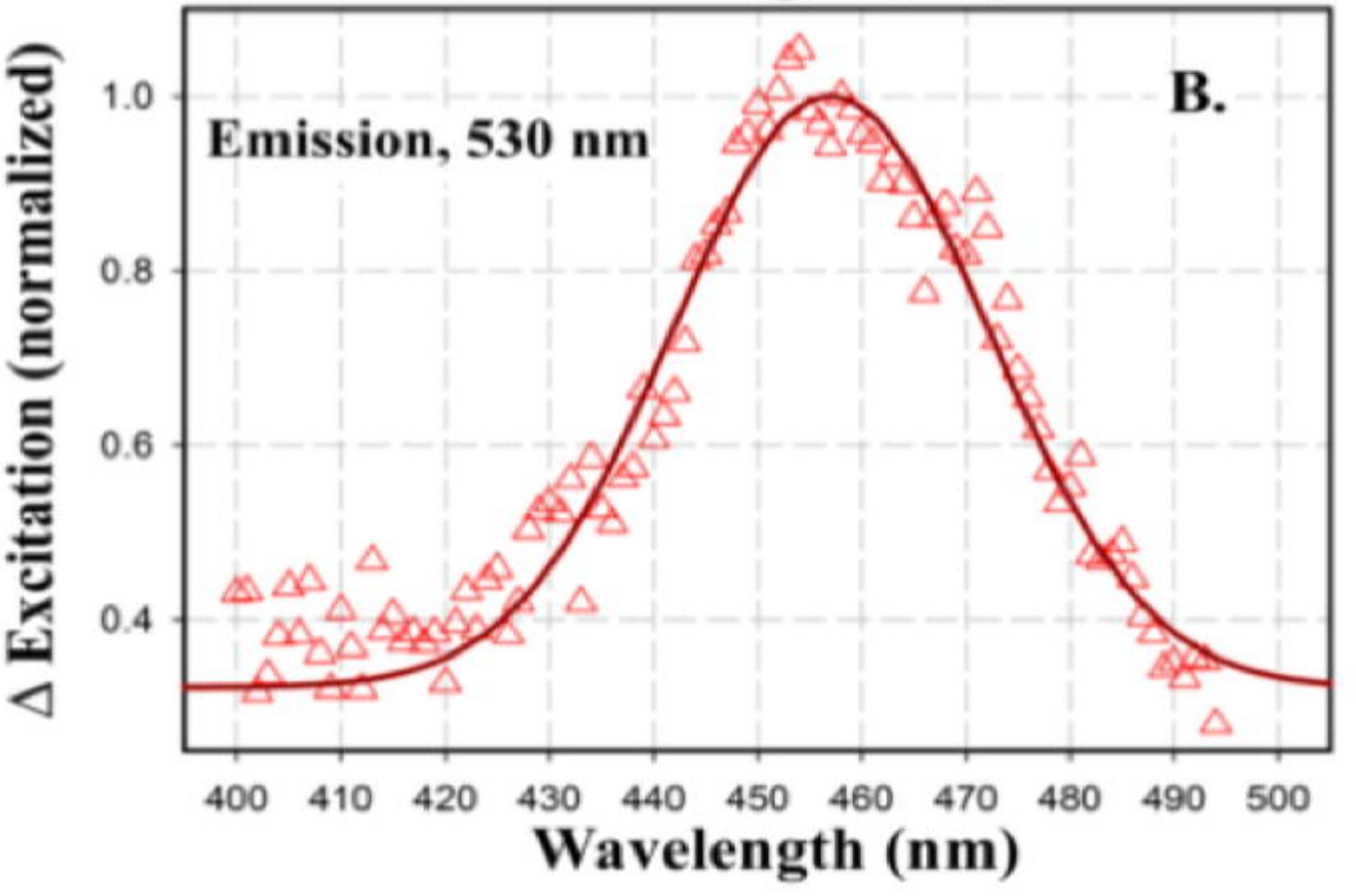
B.
Emission, 530 nm
Δ Excitation (normalized)
1.0
0.8
0.6
0.4
400
410
420
430
440
450
460
470
480
490
500
Wavelength (nm)